Eur. Phys. J. B **52**, 305–309 (2006)
DOI: 10.1140/epjb/e2006-00299-1

THE EUROPEAN PHYSICAL JOURNAL B

Tunneling magnetoresistance in small dot arrays with perpendicular anisotropy

L.F. Zhang[1], C. Xu[1,a], P.M. Hui[2], and Y.Q. Ma[3]

[1] Department of Physics, Suzhou University, Suzhou 215006, P.R. China
[2] Department of Physics, The Chinese University of Hong Kong, Shatin, New Territories, Hong Kong
[3] National Laboratory of Solid State Microstructures, Nanjing University, Nanjing 210093, P.R. China

Received 25 November 2005 / Received in final form 17 May 2006
Published online 31 July 2006 – © EDP Sciences, Società Italiana di Fisica, Springer-Verlag 2006

Abstract. The tunneling magnetoresistance (TMR) of a small magnetic dot array with perpendicular anisotropy, is studied by using a resistor network model. Because of the competition between dipolar interaction and perpendicular anisotropy, the TMR ratio can be up to a maximum value (∼26%) as predicted by a theoretical model. At moderate dipolar interaction strength, the perpendicular TMR ratio exhibits abrupt jumps due to the switching of magnetic moments in the array when the applied field (normal to the array plane) decreases from a saturation field. This novel character does not occur if the dipolar interaction between particles is quite strong. Furthermore, the effect of the array size N on TMR is also studied and the result shows that TMR ratio fluctuates when N increases for a moderate dipolar interaction strength. When the applied field h_e is parallel to the array plane, the in-plane TMR curve seems insensitive to the dipolar interaction strength, but the maximum TMR ratio (∼26%) can also be obtained at $h_e = 0$.

PACS. 75.47.-m Magnetotransport phenomena; materials for magnetotransport – 75.60.Jk Magnetization reversal mechanisms – 75.50.Tt Fine-particle systems; nanocrystalline materials

Periodic arrays of single-domain magnetic dots are of substantial interest for applications in future ultrahigh-density magnetic storage media and magnetic field sensors [1–5]. In such arrays, each nanoparticle may be viewed as a giant magnetic dipole. One key issue in the research effort on magnetic nanoparticle arrays is to understand the hysteretic behaviour and the underlying magnetization reversal mechanism. Due to the high density, small particles with a high aspect ratio and a large perpendicular anisotropy are needed for thermal stability of the magnetization state (superparamagnetic limit) [6,7]. In these patterned arrays, the dipolar fields may be comparable to bulk anisotropy fields due to the high density of magnetic particles and therefore have the potential to strongly affect static magnetic order and magnetization process. Much experimental work and various numerical studies have focused on the ground state configuration and the hysteretic behaviour of dipolar interacting nanoparticle arrays [1–5]. In our previous work, we studied the interplay between dipolar interactions and perpendicular anisotropy in small dot arrays [5]. The dipolar interaction between particles tends to keep some moments in the opposite direction to the majority, although all the moments are pointing perpendicularly to the array [5]. At a certain dipolar interaction strength, an out-of-plane antiferromagnetic (OAF) configuration will occur. In the case of very strong interactions, the out-of-plane magnetization of the nanoparticles reorients to an in-plane direction. However, it will not occur in small dot arrays with a large perpendicular anisotropy.

For such patterned nanoparticle arrays, much research work has been done in order to understand the magnetic properties. However, only a little work has studied the magnetotransport in patterned media [8,9]. Because of the insulating nature between neighbouring particles, which prevents electron transfer between neighbouring nanoparticles, the conductivity of patterned media is dominated by an electron tunneling or hopping mechanism. For example, the conductivity of a cobalt nanoparticle self-assembled film leads to a large (∼10%) tunneling magnetoresistance (TMR) at low temperature [8]. Tunneling magnetoresistance was first found by Julliere [10] in 1975, where a classical theory for tunneling was suggested based on the conduction-electron spin-polarization values (P_1 and P_2) of the FM(ferromagnet) electrodes, giving the tunneling magnetoresistance

$$\mathrm{TMR} = (R_a - R_P)/R_a = 2P_1P_2/(1 + P_1P_2). \quad (1)$$

Here R_P and R_a are the resistances with magnetizations of the electrodes parallel and antiparallel, respectively. For

[a] e-mail: cxu@suda.edu.cn

a Fe-Co tunnel junction, with P of 40% and 30%, respectively, for the two FM's, the above expression gives a 24% change in the tunneling resistance between the antiparallel and parallel orientations of M in the two FM electrodes. In tunnel-type magnetic nanostructures, the charge transport is caused by tunneling through insulating barriers. Electron tunneling depends on the relative orientation of magnetic moments between ferromagnetic granules. The tunneling resistance decreases when the magnetic moments of the granules are aligned in parallel in an applied magnetic field. For patterned nanoparticle arrays, the transport of electrons involves a number of granules, and the moments of the granules interact via dipole forces. In this system, magnetic-moment configurations of the array are dominated by the competition of the anisotropy energy, dipolar interaction energy and Zeeman energy. Especially for small arrays, magnetic-moment configurations are sensitive to the strength of the dipolar interaction between particles, and the system exhibits unusual magnetization dynamics [5]. Thus, driven by the applied magnetic field, the unusual magnetization processes are expected to cause the novel magnetoresistance phenomena in these small patterned arrays.

We assume the cylindrical dots to be arranged in a square lattice. The identical dots are considered as single-domain magnetic nanoparticles with their easy axes normal to the array plane, and they interact via dipolar forces. When an external magnetic field is applied to such an array, the magnetic moments of the particles may reorientate due to the competition between the dipolar interaction, anisotropy energy, and Zeeman energy. To obtain the equilibrium magnetic-moment configuration, we define the position of the ith dot by a position vector $\mathbf{r}_i = \hat{x}pa + \hat{y}qa$ where a is the lattice spacing and p and q are integers. The motion of the magnetic moment $\mathbf{m}$ in the array can be described by the LLG equation

$$\frac{d\mathbf{m}_i}{dt} = -\gamma \mathbf{m}_i \times \mathbf{H}_i + \frac{\alpha}{m}\mathbf{m}_i \times \frac{d\mathbf{m}_i}{dt}, \tag{2}$$

where γ is the gyromagnetic ratio, and α controls the rate of dissipation. The local magnetic field $\mathbf{H}_i$ at site $\mathbf{r}_i$ includes the external magnetic field $\mathbf{h}_e$, the dipolar field $\mathbf{h}_{dip}$ and a single-particle effective anisotropy field perpendicular to the array given by $km_{zi}\hat{z} = (2K/M_s)m_{zi}\hat{z}$, where K is the anisotropy energy and M_s is the saturated magnetization of the particle and $m_{zi} = \cos(\mathbf{m}, \hat{z})$. With these definitions, the field $\mathbf{H}_i$ is given as

$$\mathbf{H}_i = \mathbf{h}_e + \mathbf{h}_{dip} + km_{zi}\hat{z}, \tag{3}$$

where the dipolar field can be written as

$$\mathbf{h}_{dip} = h_d M_s \sum_{j\neq i} \frac{3(\hat{\mathbf{r}}_{ij}\cdot\hat{\mathbf{m}}_j)\hat{\mathbf{r}}_{ij} - \hat{\mathbf{m}}_j}{\tilde{r}_{ij}^3}, \tag{4}$$

where $h_d = V/a^3$, V is the volume of a particle, $\hat{\mathbf{r}}_{ij}$ is the unit vector pointing from dipole moment $\mathbf{m}_i$ to $\mathbf{m}_j$, and $\hat{\mathbf{m}}_j$ is the unit vector of moment $\mathbf{m}_j$, and $\tilde{r}_{ij} = r_{ij}/a$. Inspection of equation (2) shows that it can be written in spherical coordinates involving only two degrees of freedom for each dot. The problem is then treated by numerically solving the set of $2N^2$ coupled equations for a square dot array of dimension N using the four-order Runge-Kutter method [5].

For a given magnetic-moment configuration $\{\mathbf{m}_i\}$ of the nanoparticle array, we use a resistor network model [11] to study the TMR effect. Due to the spin-dependent tunneling, the conductance between two separated nanoparticles i and j can be written as [8,9,12]

$$\sigma_{ij} \propto \left(1 + P^2\cos\theta_{ij}\right)\ \exp(-r_{ij}/\lambda - E_c/k_BT), \tag{5}$$

where P is the spin polarization, θ_{ij} is the relative angle between neighbouring moments, $E_c = e^2/2C$ is the activation energy to charge a neutral nanoparticle by the addition of a single electron, C is the nanoparticle capacitance relative to its surrounding medium, and $\lambda = \hbar/\sqrt{8m^*(U - E_F)}$ is the decay length of the electron wave function in the insulating barrier of height U relative to the Fermi energy E_F, m^* is the effective mass of electrons. In all our simulations, we assumed $\lambda = a$, as a sufficient requirement to allow charge transfer between neighbouring nanoparticles and assumed $P = 0.34$ corresponding to the value of a cobalt nanoparticle [8,9,13]. The form of equation (5) predicts a linear behaviour of $\ln\sigma$ vs. $1/T$ for nanoparticles with a negligible size dispersion, which was observed in a recent experiment [8]. In this paper, we focus on the effect of the magnetic-moment configuration on the TMR ratio, thus we take T as a constant in our calculation. Equation (5) neglects the magnetic exchange energy E_M, which was considered by Inoue and Maekawa [12] and has a negligibly small contribution for cobalt nanoparticles at low temperatures. Thus, we expect that the contribution of E_M to TMR in our model is small, and that it can be neglected. Inspection of equation (5) suggests that the orientations of neighbouring magnetic moments will affect the conductance between them. Consequently, the system's conductance σ will be dependent on the magnetic-moment configuration of the array. Therefore, it causes the TMR effect after we apply an external magnetic field h_e to the array. The TMR ratio is defined by

$$\mathrm{TMR}(\mathbf{h_e}) = \frac{\sigma(\mathbf{h_s}) - \sigma(\mathbf{h_e})}{\sigma(\mathbf{h_e})}, \tag{6}$$

where $\mathbf{h_s}$ is the saturation field which makes all the magnetic moments orientate along it. By considering equations (5) and (6), one can immediately get a theoretical maximum TMR ($=2P^2/(1-P^2)$) if spin electrons only transfer between nearest neighbours. In our model, the theoretic maximum TMR ratio is about 0.26 for $P = 0.34$.

The system's conductance is calculated in the following way: we start with a square lattice array, where each site represents a magnetic moment (see Fig. 1). Between the nearest neighbour sites, we insert a resistor, whose conductance (or resistance) is phenomenologically expressed by equation (5). The total conductance (or resistance) is

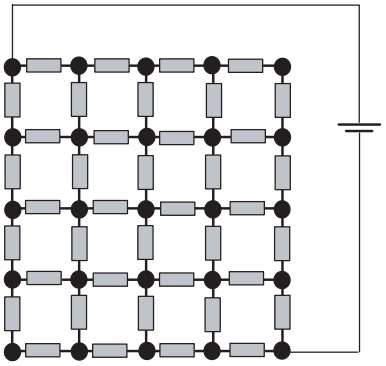

Fig. 1. An example of the construction of a resistor network with particles distributed on a square lattice.

calculated with the framework of RN. For a small magnetic dot array, we use free boundary conditions, and the voltage is applied to two nanoparticles on the diagonal of the array. We assume that the spin-dependent electrons only transfer between the nearest neighbour sites, that is, we insert a resistor only between the nearest neighbour sites. The TMR ratio is obtained after the magnetic moments reach the equilibrium state at a given h_e. In all the calculations, we take $k/M_s = 4.0$ and $\alpha = 0.2$.

1 Results and discussion

The TMR ratio as a function of the applied magnetic field, which is normal to the array plane, is shown in Figure 2 for two different dipolar interaction strengths. Two configurations **A** and **B** of the moments corresponding to the plateaus in the perpendicular TMR are shown in the inset of Figure 2a, where the arrow head indicates the orientation of a magnetic moment. It means that, when the magnetic-moment configuration changes from the initial saturation configuration (all the moments in the $+z$-direction) into configuration A or B, the TMR ratio is about 13% or 26%. In small arrays, it can be seen that the TMR ratio is closely related to the magnetic-moment configurations. It is worth noting that, the jumps in Figure 2 correspond to the evolution of the magnetic-moment configurations. For example, when $h_e/M_s = -1.8$, by comparing with the case of configuration B, the configuration A has four moments flipped which are located at the four corners of a 5×5 array and hence the TMR ratio jumps from $\sim$13% to $\sim$26%. The evolution of the magnetic-moment configuration is caused by the competition between the anisotropy energy, the dipolar interaction and the Zeeman energy. Since the uniaxial anisotropy lowers the energy of the moments if they align perpendicularly to the array, configurations with the moments pointing at any polar angles other than $\theta \approx 0$ and $\theta \approx \pi$ have higher energies. Thus, for a moment to flip from the $+z$-direction to $-z$-direction, it needs to pass over an energy barrier. Only when the external field reaches a certain value will the energy barrier be surpassed with the assistance of the Zeeman energy [14]. Thus, some moments of the array flip when h_e decreases from an initially saturated field

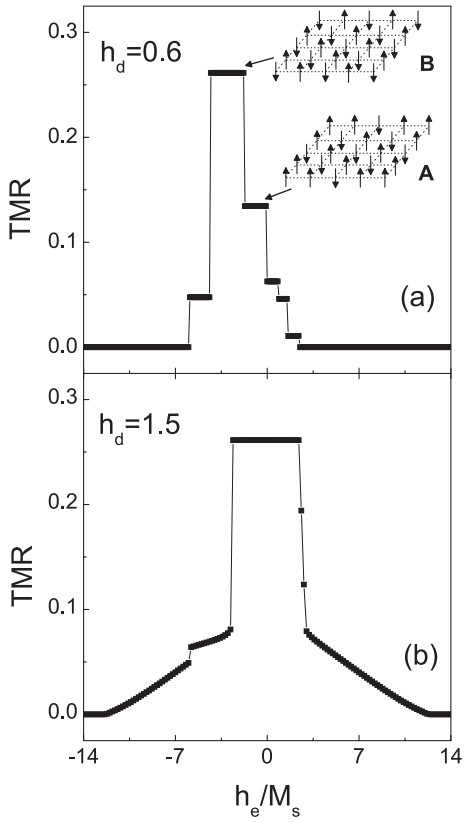

Fig. 2. The TMR ratio as a function of the applied magnetic field normal to the array plane for a 5×5 dot array with $h_d = 0.6$ and $h_d = 1.5$. The magnetic-moment configurations **A** and **B** corresponding to the TMR ratios 0.13 and 0.26, respectively, are also shown in the sketches.

h_s (shown in Fig. 2a), which results in a sudden change of the values of some resistor bars in the RN and hence the jumps occur. This feature is quite different from those in randomly distributed granular composites [15] or polycrystalline compounds [16]. Based on equation (5), σ_{ij} is low if the two moments of the particles i and j are antiparallel to each other, while it is high if they are parallel to each other. Therefore, when some of the moments switch as h_e decreases, the number of high-value resistors increases in the RN and hence the total resistance of RN becomes high, which causes the increase in the TMR ratio. Obviously, if the magnetic moments can be in an antiparallel state at certain h_e, the TMR ratio will be maximum according to equation (5). In our model, the maximum TMR ratio ($\sim$0.26) predicted by theoretical calculation can be obtained since the OAF state is realized within a certain range of h_e (illustrated by **B** in Fig. 2a). The maximum TMR ratio is larger than that obtained in a random anisotropy dot array (about 0.1) [9]. For larger h_d (see Fig. 2b), the maximum TMR again can be reached due to the antiparallel orientations of magnetic moments. However, the many small drops disappear in comparison with Figure 2a. This is due to the strong dipolar interaction for which there is no longer any restriction that the magnetic moments be normal to the array plane when the

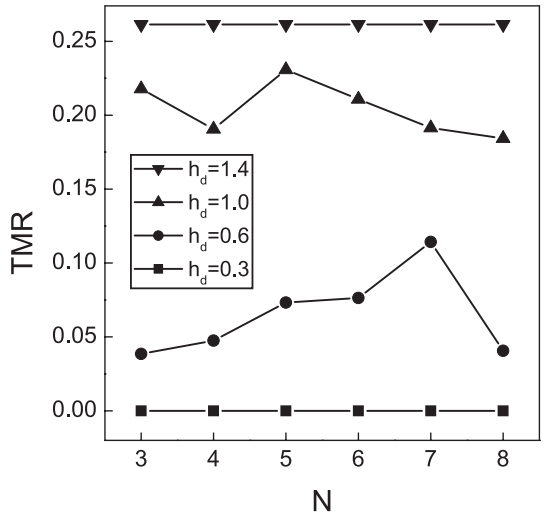

Fig. 3. The values of TMR as a function of array size N with different dipolar interaction strengths.

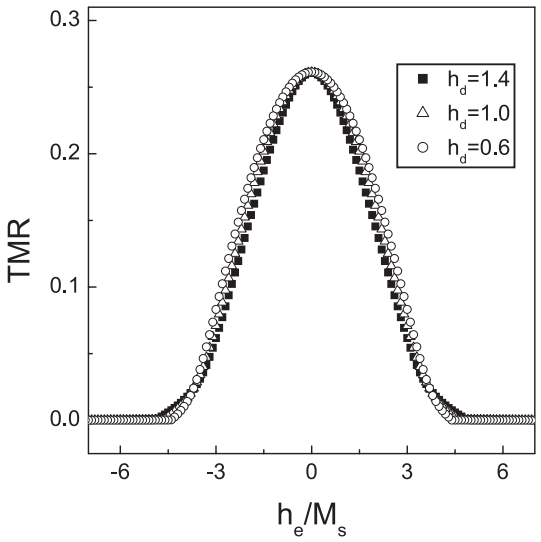

Fig. 4. The TMR ratio as a function of the applied magnetic field parallel to the array plane for a 5×5 dot array at different dipolar interaction strengths.

configuration is not in an antiferromagnetic state. Thus, the TMR curve tends to look smoother than that in Figure 2a. Note that, the TMR curve is not symmetric in terms of h_e, meaning that the TMR shows hysteresis behaviour when one applies an external field normal to the array plane.

As discussed above, the magnetic-moment configuration greatly affects the TMR ratio. In our previous work [5,14], we found that the size of the small dot array is important to the formation of an equilibrium configuration at a certain dipolar interaction strength. Therefore, it is necessary to investigate the influence of array size and dipolar interaction on the perpendicular TMR. The result is shown in Figure 3. Here the TMR ($h_e = 0$) is obtained by switching off h_e from h_s to zero directly. There are two limiting cases for which the TMR is independent of the size of the small dot array. One limiting case is the weak dipolar interaction. In our model, when $h_d \leq 0.3$, the TMR is approximately equal to zero. It indicates that the saturated magnetic-moment configuration (with all the moments pointing along $+z$-direction) does not change when the saturated field h_s becomes zero. In this weak dipolar interaction region, the magnetic moment in the array behaves similarly to an isolated moment. Due to the large perpendicular anisotropy, all the magnetic moments still point along $+z$-direction as $h_e = 0$. Therefore, the TMR ratio is zero. The other limiting case is the strong dipolar interaction. When $h_d \geq 1.4$, the TMR reaches the theoretically predicted maximum value ($\sim$0.26) at $h_e = 0$. It means that the strong dipolar interaction between particles forces the magnetic moments into an OAF configuration when h_e is zero. In this dipolar region, the anisotropy energy barrier can be overcome due to the interaction between particles and the collective behaviour of the particles are apparent. The magnetic moments can tune themselves to an OAF configuration in terms of the strong dipolar interaction. Therefore, the TMR ratio reaches a maximum value and becomes independent of the array size. However, when the dipolar interaction strength is moderate, in the region $0.3 < h_d < 1.4$, the array size N significantly affects the TMR ratio. In Figure 3, we give two values of h_d as examples. The fluctuation of TMR indicates that the magnetic-moment configuration varies for different N though the dipolar interaction strength between the moments is fixed. To obtain the final magnetic-moment configuration, the competition between the long-range dipolar interaction and anisotropy energy should be considered. More details can be found in references [5] and [14].

The TMR ratio as a function of the applied magnetic field, which is parallel to the array plane, is shown in Figure 4. It seems that the in-plane TMR curves are insensitive to the dipolar interaction strength, which is different from the perpendicular TMR (shown in Fig. 2). As the applied field gradually decreases from a saturation field h_s, the magnetic moments will gradually transit from an in-plane orientation to an out-of-plane orientation. This smooth transition is tuned by the coupled dipolar field. While the nanoparticle has its easy axis normal to the array plane, the dipolar interaction will force the neighbouring moments in opposite directions so as to reduce the total energy. Thus, when h_e gradually decreases to zero, the magnetic-moment configuration will evolve into the OAF configuration and the value of TMR will reach a maximum. We also note that the in-plane TMR ratio is almost independent of the array size.

In summary, the TMR effect exhibits a close much dependence on the magnetic-moment configuration, which is tuned by the dipolar interaction in small magnetic dot arrays. The dipolar interaction prefers the magnetic moments to form an OAF configuration in strong perpendicular anisotropy dot arrays and the TMR ratio can be up to a theoretically predicted maximum ($\sim$0.26). The perpendicular TMR shows abrupt jumps due to the switching of the magnetic moments in the array as the applied field

decreases. This novel feature may be useful for applications. The perpendicular TMR ratio shows fluctuations as the array size increases at moderate dipolar interaction strength. This fluctuation disappears in both the weak and strong dipolar interaction regions. The in-plane TMR curve seems insensitive to the dipolar interaction strength, but the maximum TMR ratio can be obtained at $h_e = 0$ for different dipolar interaction strengths.

References

1. *Magnetic Nanostructures*, edited by H.S. Nalwa (American Scientific Publishers, 2002)
2. C.A. Ross et al., J. Appl. Phys. **91**, 6848 (2002)
3. C.A. Ross et al., Phys. Rev. B **65**, 144417 (2002)
4. M.A. Kayali, W.M. Saslow, Phys. Rev. B **70**, 174404 (2004)
5. L.F. Zhang, C. Xu, P.M. Hui, Y.Q. Ma, J. Appl. Phys. **97**, 103912 (2005)
6. D. Weller et al., IEEE. Trans. Magn. **36**, 10 (2000)
7. D.N. Lambeth, E.M.T. Velu, G.H. Bellesis, L.L. Lee, D.E. Laughlin, J. Appl. Phys. **79**, 4496 (1996)
8. C.T. Black, C.B. Murray, R.L. Sandstrom, S. Sun, Science **290**, 1131 (2000)
9. D. Kechrakos, K.N. Trohidou, Phys. Rev. B **71**, 054416 (2005)
10. M. Julliere, Phys. Lett. A **54**, 225 (1975)
11. C. Xu, P.M. Hui, Z.Y. Li, J. Appl. Phys. **90**, 365 (2001)
12. J. Inoue, S. Maekawa, Phys. Rev. B **53**, R11 927 (1996)
13. P. Meservery, P.M. Tedrow, Phys. Rev. B **7**, 318 (1973)
14. C. Xu, P.M. Hui, L.F. Zhang, Y.Q. Ma, J.H. Zhou, Z.Y. Li, Eur. Phys. J. B **46**, 475 (2005)
15. T. Zhu, Y.J. Wang, Phys. Rev. B **60**, 11918 (1999)
16. H.Y. Hwang, S.-W. Cheong, N.P. Ong, B. Batlogg, Phys. Rev. Lett. **77**, 2041 (1996)